

Mechanical Surface Treatment of Cold-Extruded Workpieces [†]

Peter Herrmann ^{1,*} , Martina Müller ¹, Ingo Felix Weiser ¹, Tim Herrig ¹ and Thomas Bergs ^{1,2}

¹ Laboratory for Machine Tools and Production Engineering WZL (Werkzeugmaschinenlabor), RWTH Aachen University, Campus-Boulevard 30, 52074 Aachen, Germany

² Fraunhofer Institute for Production Technology, Steinbachstraße 17, 52074 Aachen, Germany

* Correspondence: p.herrmann@wzl.rwth-aachen.de

[†] Presented at the 28th Saxon Conference on Forming Technology SFU and the 7th International Conference on Accuracy in Forming Technology ICAFT, Chemnitz, Germany, 2–3 November 2022.

Abstract: Cold-forming processes represent important technologies in steel processing. Cold-formed workpieces are often case-hardened in an energy- and cost-intensive process. Alternative finishing can be carried out by means of mechanical surface treatments, such as deep rolling or machine hammer peening. Since the limitations of deep rolling of cold-formed workpieces have been insufficiently explored, this work investigates cause-and-effect relationships between the process parameters of full forward extrusion and deep rolling and the resulting surface integrity. For the experimental investigation, the material 16MnCr5 is used. The focus of the workpiece analysis is on the resulting residual stresses, hardness, and roughness.

Keywords: cold forming; impact extrusion; surface integrity; deep rolling; residual stress

1. Introduction

Due to high material and energy efficiency, cold-forming processes represent an important area in the processing of steel. In particular, impact extrusion operations are additionally characterized by high dimensional and shape accuracy, good surface qualities, favorable, continuous fiber flow, as well as positive strain-hardening conditions [1]. To improve wear and fatigue resistance without affecting the initially soft and tough interior, case-hardening of the components produced by full forward extrusion (FFE) is usually applied [2]. The use of case-hardened steel is particularly advantageous because its low carbon content qualifies it for cold-forming and at the same time the prerequisites for hardening the edge zone are fulfilled [3].

In addition to case-hardening, the fatigue resistance of the shaft component surface may be improved by mechanical surface treatments such as deep rolling [4], machine hammer peening [5], and shot peening [6]. Deep rolling is a widely used industrial manufacturing process based on the plastic deformation of metallic surfaces [7]. The process is mainly used to increase the lifetime of dynamically loaded components such as shouldered shafts or crankshafts [8]. The main reasons for the increase in lifetime are the smoothing of micro-notches on the surface, work-hardening of the edge zone, and the introduction of compressive residual stresses [4]. Additionally, grain refinement of the near-surface edge zone occurs during deep rolling [9].

As case-hardening is an energy-intensive process and is associated with costly subsequent work due to thermal distortion, there is a demand for alternative production chains. Among other things, the combination of cold-forming and mechanical surface treatments without hardening is an attractive option [10]. The positive workpiece properties after impact extrusion are retained, while incremental forming can increase wear and fatigue resistance. A concrete example is represented by the assembled gear shaft. In this case, the shaft body and gearing are manufactured separately and the components are subsequently joined. The hardening process is only performed on the gearing components and therefore



Citation: Herrmann, P.; Müller, M.; Weiser, I.F.; Herrig, T.; Bergs, T. Mechanical Surface Treatment of Cold-Extruded Workpieces. *Eng. Proc.* **2022**, *26*, 24. <https://doi.org/10.3390/engproc2022026024>

Academic Editors: Martin Dix and Verena Kräusel

Published: 25 November 2022

Publisher's Note: MDPI stays neutral with regard to jurisdictional claims in published maps and institutional affiliations.



Copyright: © 2022 by the authors. Licensee MDPI, Basel, Switzerland. This article is an open access article distributed under the terms and conditions of the Creative Commons Attribution (CC BY) license (<https://creativecommons.org/licenses/by/4.0/>).

less energy-intensive. The basic shaft body can be produced without hardening using a combination process of full forward extrusion (FFE) and deep rolling [10].

For the design of the deep rolling process of an impact extruded component, there is a considerable deficit of scientific knowledge about the concrete cause–effect relations between process parameters and surface integrity as well as component performance. In contrast to previously hardened workpieces, where the Hertzian pressure in the contact between tool and workpiece is often used as a parameter for process design [11], Hertzian pressure cannot be used in this case due to the too-soft workpiece [12]. In addition, the deep rolling process considered here can only be partially compared with the deep rolling of milled workpieces. The reason is that the forming capacity of the material is already largely exhausted and surface cracks and spalling occur even at low rolling forces [10].

The ability to modify the surface properties of full forward extruded workpieces by deep rolling is demonstrated in this paper for the 16MnCr5 material. For this material, research results regarding the first process step, which is full forward extrusion, are already available. It was found that the triaxiality during the forming process is the main factor influencing damage accumulation. High triaxiality leads to damage accumulation, while a low triaxiality prevents the development of damage [13]. Contrary to the expectation, higher strain does not inevitably lead to more damage [14].

2. Materials and Methods

Mechanical surface treatments offer potential regarding the optimization of cold-formed components. The state of the art shows that the cause–effect relationships between deep rolling parameters and the resulting surface integrity are different for the machining of full forward extruded workpieces than for the machining of hardened workpieces. However, knowledge of the interrelationships is indispensable for a reliable process design. Therefore, an experimental study was performed on the 16MnCr5 material (1.7131/AISI 5115).

2.1. Setup for Full Forward Extrusion

In the initial state, the workpiece is cylindrical (diameter $d_0 = 30$ mm, length $l = 71$ mm), and the edge of the lower face is provided with a radius $r_0 = 3$ mm. The entire surface was initially roughened by shot peening, phosphate, and lubricated with GARDOMER L 6444-1. The impact extrusion was carried out on a hydraulic press from SCHULER (SCHULER PRESSEN GMBH, Göppingen, Germany), model HPX400, with a maximum pressing force $F_{\text{Press}} = 4000$ kN. The punch force was recorded piezoelectrically. The tool setup in the hydraulic press and a schematic representation of full forward extrusion (FFE) including the relevant process parameters are shown in Figure 1. Figure 1a shows the test setup inside the SCHULER HPX 400.

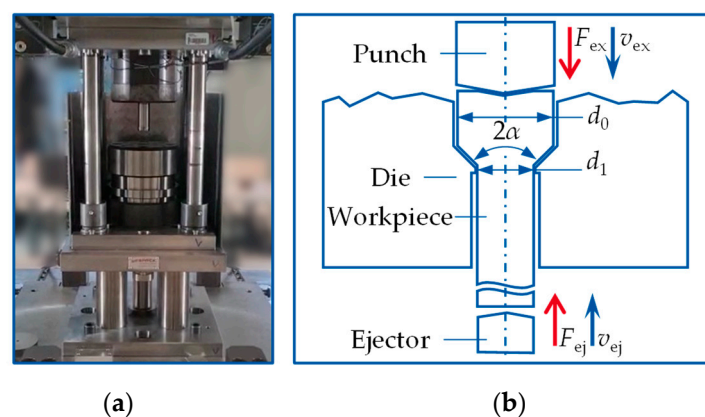


Figure 1. (a) Tool setup inside the SCHULER HPX400 and (b) schematic representation of full forward extrusion.

The FFE consists of the two substeps, extrusion and ejection, whereby the workpiece is first pressed almost completely through the die by the punch and then ejected in the opposite direction by the ejector. In Figure 1b, in addition to the geometrical parameters (initial diameter d_0 , shoulder diameter d_1 , and shoulder opening angle 2α), the forces of punch F_{ex} and ejector F_{ej} , as well as the velocities of punch v_{ex} and ejector v_{ej} are specified. To establish comparability with other series of tests carried out at the WZL, the diameters were set to $d_0 = 31.4$ mm and $d_1 = 20.6$ mm. For the shaft shoulder formed during FFE, this results in a length of 100 mm. Since larger shoulder opening angles cause a greater logarithmic strain in the near-surface edge zone and exhaustion of the forming capacity before deep rolling must be avoided, a shoulder opening angle of $2\alpha = 60^\circ$ was selected. The process velocities were set to $v_{ex} = v_{ej} = 10$ mm/s.

All tests were carried out at room temperature without active heating of die, punch, or ejector. Since these elements also heat up during cold forging and because this affects the process, the tool temperature was set to a steady-state value by repeating the process on several specimens. The maximum punch force of each impact extrusion process was used to check at what point steady-state conditions occurred. The course of the maximum punch force is shown in Figure 2 above the test number.

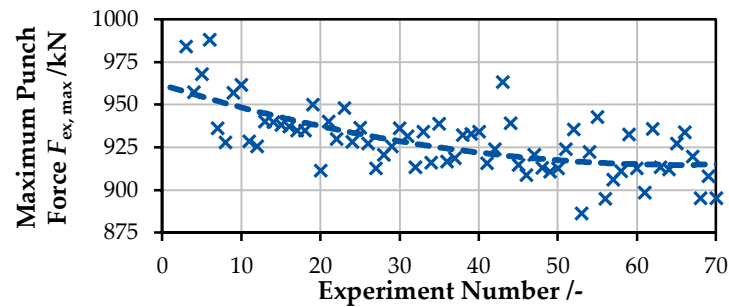


Figure 2. Development of maximum punch force during repeated full forward extrusion tests.

As shown in Figure 2, the maximum punch force decreases with increasing number of tests. After 60–70 tests, the punch force reaches a saturation value of $F_{ex,max} = 915$ kN. The conditions are considered constant from this point on, even though $F_{ex,max}$ continues to vary by up to 20 kN around this saturation value.

2.2. Deep Rolling Setup

In the tests carried out, a hydrodynamic deep rolling tool from ECOROLL (ECOROLL AG, Celle, Germany) was used in combination with a conventional lathe. Figure 3 shows the schematic setup of the test execution and the deep rolling tool.

Figure 3a shows the test setup consisting of workpiece and deep rolling tool. The workpiece is guided on the lathe and rotates at the speed n . The tool is moved parallel to the workpiece axis at the feed rate v_f . The step over distance s between two rolling paths on the specimen is $s = v_f/n$.

Figure 3b shows the properties of the hydrodynamic deep rolling tool. The rolling ball can be moved dynamically around the infeed i during the process. This ensures that the rolling ball and the workpiece are in continuous contact during the process. The rolling force F_{dr} shown on the right side of the figure results from the linear correlation:

$$F_{dr} = A_b \cdot p_{dr} \cdot (1 - \delta) \quad \text{with } A_b = r_b^2 \cdot \pi. \quad (1)$$

The parameter δ denotes the pressure loss in the system and equates to 0.2969 for the ball with $r_b = 6.5$ mm.

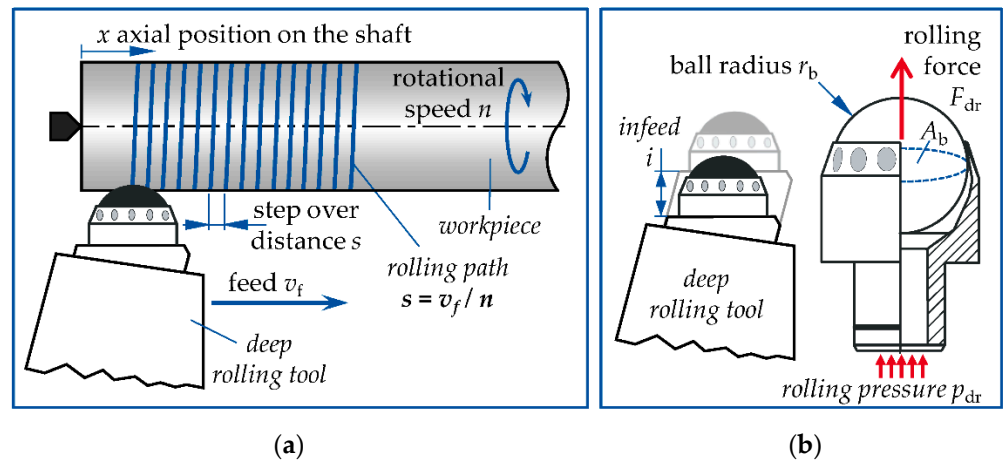


Figure 3. (a) Test setup including tool and workpiece and (b) properties of the hydrodynamic deep rolling tool from the ECOROLL AG according to [15].

In a test series at other research institutions, no hardness increase could be achieved for impact-extruded 16MnCr5 by means of hydrodynamic deep rolling [10]. In the tests carried out there, deep rolling forces of up to 550 N and an exclusive ball diameter $d_b = 6$ mm were used. These research results were initially confirmed in preliminary tests carried out at WZL. In addition, it was found that when using the ball diameter $d_b = 13$ mm, surface spalling only occurs with rolling pressure $p_{dr} \approx 20$ MPa $\hat{=}$ 1866 N.

2.3. Test Design

The overarching purpose is to increase the strength of 16MnCr5 workpieces produced by full forward extrusion by means of deep rolling. Since strength investigations—especially for concrete applications—involve a large amount of effort, it must first be demonstrated that the modification of hardness, roughness, and/or residual stress state can be achieved by deep rolling. To reach this objective, two experimental deep rolling setups were created, the parameters of which are presented in Table 1. The two deep rolling tests are compared with both the workpiece condition after full forward extrusion (FFE) and the corresponding ejection process and after FFE before the corresponding ejection process.

Table 1. Process parameters for the machining of the four specimens investigated.

Specimen/ Process Parameter	FFE before Ejection	FFE after Ejection	Setup A	Setup B
Shoulder opening angle $2\alpha/^\circ$	60	60	60	60
Extrusion and ejection velocity $v_{ex} v_{ej}/(\text{mm/s})$	10	10	10	10
Ball diameter d_b/mm	-	-	13	13
Rolling pressure p_{dr}/MPa	-	-	15	10
Rolling Force F_{dr}/N	-	-	1400	933
Step over distance s/mm	-	-	0.05	0.2
Rotational speed $n/(1/\text{min})$	-	-	398	398

All four samples were processed with the same FFE parameters. To produce the specimen manufactured without ejection, the FFE process was stopped and the end protruding from the die was separated from the specimen part in the die by means of erosion. After the FFE, the lubricant was removed manually with a highly alkaline cleaner.

To detect modification of the edge zone, a rolling force as large as possible was selected in Setup A, at which it was found in preliminary tests that no surface spalling occurs. With the aim of achieving a high surface quality, a small step over distance $s = 0.05$ mm was selected at the same time. To achieve a lower energy input in the second setup, Setup B,

than in Setup A, a significantly lower rolling force and an increased step over distance s were set.

2.4. Measurement Methods and Objectives

After the tests, roughness measurements were performed according to EN ISO 25178 and waviness parameters were determined according to VDA 2007. The roughness was described using the surface parameters S_a (arithmetical mean height of the surface) and S_z (maximum height of the surface). The waviness parameters WD_{sm} (mean period length of the dominant waviness) and WD_c (mean profile height of the dominant waviness) were determined. The measuring method used was the profile method on a MAHR LD 260 equipped with a MAHR LP C 45-20-5/90° probe. The Vickers HV5 hardness tests were carried out on a ZWICKROELL ZHU 250 tester (ZWICKROELL GMBH & CO. KG, Ulm, Germany) in accordance with EN ISO 6507. For statistical validation, the results of the impact extruded specimen were documented in triplicate; those of Setup A and B were measure six times. In order not to modify the surface condition, the surfaces were not ground for the test. The residual stress states were determined using ESPI (electronic speckle pattern interferometry) on a PRISM 2 from STRESSTECH (STRESSTECH GMBH, Rennerod, Germany) in each case twice. In this method, a depth profile of the residual stress state is recorded destructively by means of a borehole.

3. Results

The presentation of results is divided into three sections. First, the roughness measurements are presented, followed by hardness tests and residual stress conditions. All test results were recorded along the thin shaft shoulder at an axial position $x = 55$ mm away from the shaft end (cf. Figure 3a). When multiple results are specified, they were recorded at equal intervals along the circumference at $x = 55$ mm.

3.1. Roughness Measurements

The primary profiles in Figure 4a,b show flat grooves in the axial direction x of the specimen. These are significantly larger after ejection than before ejection, even though the profile height decreases slightly. The profile in Figure 4c is noticeably lower than the three comparisons. In contrast to Figure 4c, Figure 4d shows a clear wave structure in the tangential direction y of the specimen.

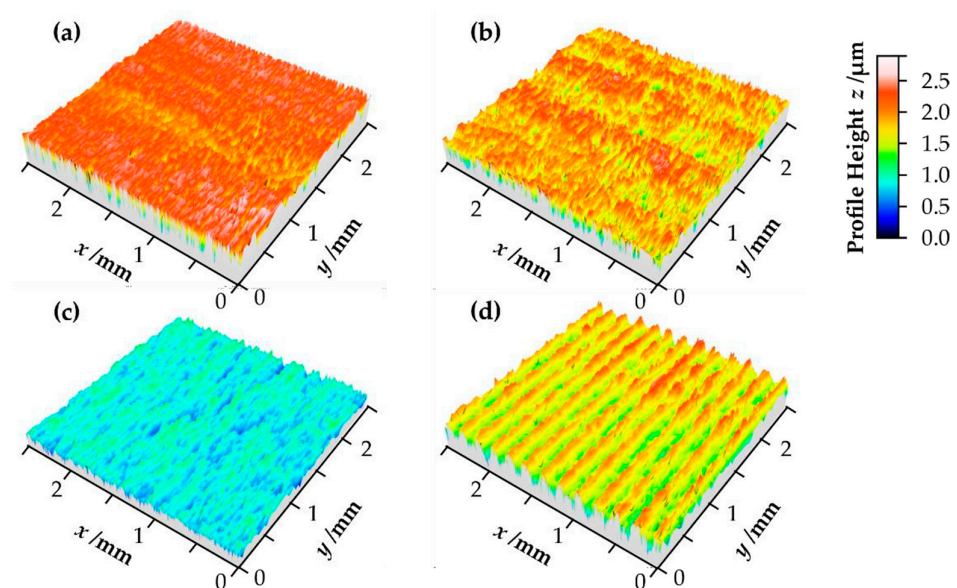


Figure 4. Primary surface profiles of the specimen (a) after full forward extrusion (FFE) before ejection, (b) after FFE including ejection, (c) after deep rolling with Setup A, and (d) after deep rolling with Setup B.

The described results can also be quantified by the determined values of the arithmetic mean height S_a and the maximum height of the surfaces S_z in Table 2. Although the values of the samples during and immediately after the FFE are in a similar range, a significant increase of the surface quality can be observed in Setup A. Such an increase can also be observed to a small extent in Setup B, even though the difference is comparatively small, particularly for S_z .

Table 2. Results of roughness and waviness measurements.

Specimen/ Surface Parameter	FFE before Ejection	FFE after Ejection	Setup A	Setup B
$S_z/\mu\text{m}$	2.81	2.68	1.38	2.63
$S_a/\mu\text{m}$	0.336	0.377	0.153	0.288
WD_{sm}/mm	0.151	0.127	0.159	0.197
Individual	0.096	0.058	0.230	0.194
WD_{sm} Results	0.108	0.260	0.112	0.200
$WD_c/\mu\text{m}$	0.250	0.064	0.134	0.196
Individual	0.462	0.548	0.209	0.617
WD_c Results	0.554	0.639	0.203	0.637
Individual	0.512	0.431	0.211	0.550
WD_c Results	0.321	0.575	0.214	0.665

For each of the waviness parameters, the three individual results from which the mean value is calculated are given separately. The large variations in these values indicate that the dominant waviness is not equally distributed throughout the specimen. For the specimens FFE before ejection, FFE after ejection and Setup A, dominant waviness cannot be clearly characterized, since as expected the mean period length in Setup A corresponds to the step over distance s . This circumstance can be seen in Setup B. The waviness is exactly determined in a range of $6\ \mu\text{m}$ and approximates to $0.2\ \text{mm}$.

3.2. Hardness Tests

The hardness values determined after full forward extrusion vary along the position on the thin shaft shoulder x in the range from $218\ \text{HV}_5$ to $310\ \text{HV}_5$ (see Figure 5a). Starting from the shaft end, the hardness increases significantly along the shoulder. The values determined at a single position x also vary by up to $56\ \text{HV}_5$ at $x = 60\ \text{mm}$.

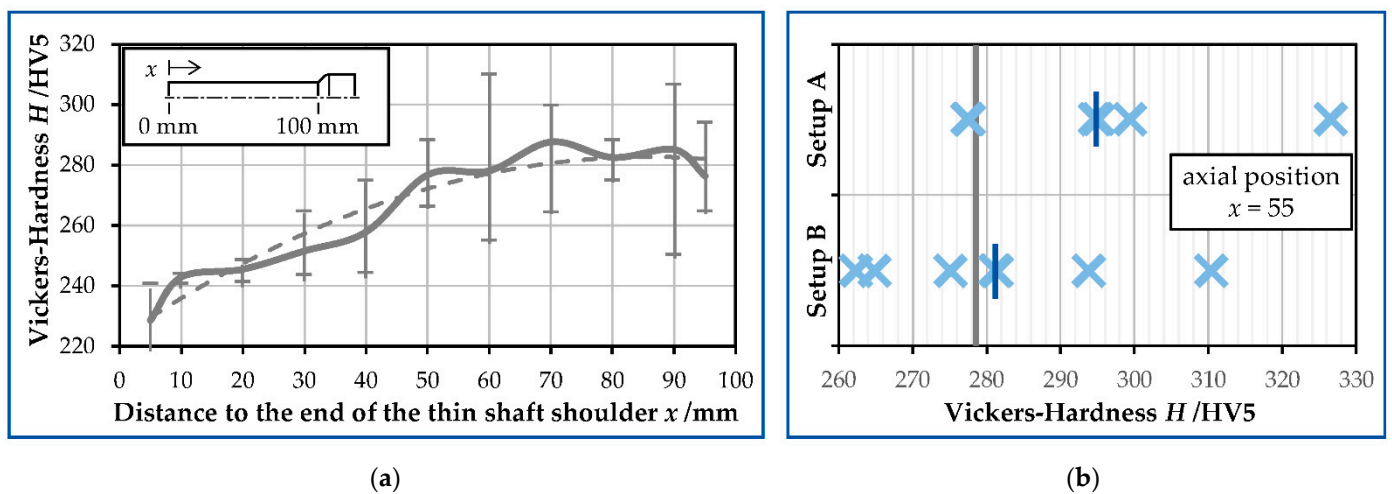


Figure 5. (a) Vickers hardness after full forward extrusion along the entire shoulder length and (b) compared to Setup A and B at position $x = 55\ \text{mm}$.

The hardness values were collected at the location $x = 55\ \text{mm}$, as were the roughness measurements and the residual stress values. The hardness comparison between the impact

extruded specimen and Setups A and B is shown in Figure 5b. For Setups A and B, six tests each were carried out, with the values of each setup varying by approximately 48 HV5. The arithmetic mean is 294.8 HV5 for Setup A and 281.3 HV5 for Setup B. Compared to the initial condition (278.7 HV5), there is a significant increase in hardness for Setup A, but a small increase in hardness for Setup B.

3.3. Residual Stress Analysis

As described in the introduction, the residual stress state of a specimen formed via full forward extrusion (FFE) is significantly modified during the ejection process. This condition is shown graphically in Figure 6. For both states, the residual stresses in axial and tangential specimen direction are shown for the axial position $x = 55$ mm. The diagrams show both the curves of the measurements performed twice and the mean value of these measurements.

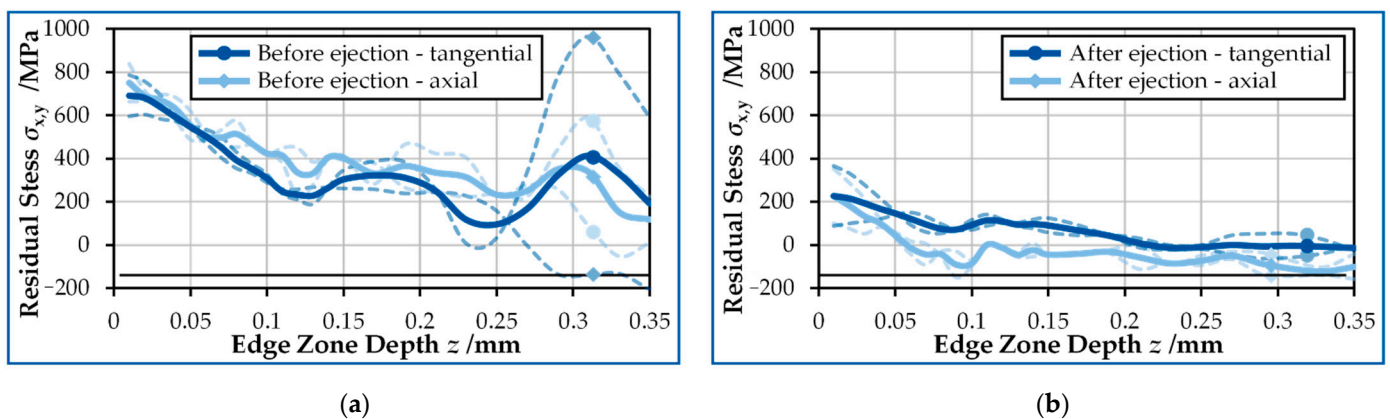


Figure 6. Residual stress states during full forward extrusion (FFE) (a) before the ejection and (b) after the ejection process.

In Figure 6a, the residual stresses in the tangential direction are initially greater than those in the axial direction. Both curves develop similarly and decrease continuously from the surface with approx. 700 MPa into the workpiece core with approx. 100–200 MPa. The strongly deviating curves from an edge zone depth of approx. 0.26 mm are to be regarded as unphysical. In Figure 6b, the residual stresses in the axial direction are noticeably larger than those in the tangential direction. The residual tensile stresses were reduced to a level below 300 MPa during the ejection process.

After deep rolling in Setups A and B, their residual stresses are similar in the axial and tangential directions. In Figure 7a,b, the compressive residual stresses in the axial direction are significantly larger in each case. For both setups, the graphs run from a level of approximately -900 to -1300 MPa at the surface to significantly lower compressive residual stresses in the core.

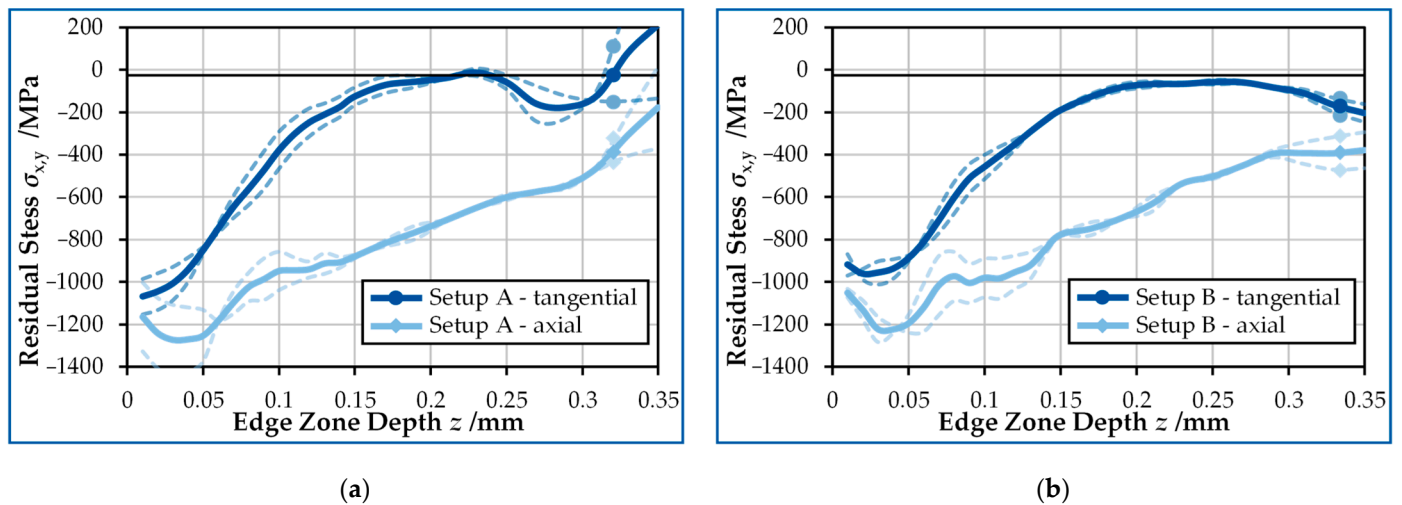


Figure 7. Residual stress state after deep rolling (a) with Setup A (b) with Setup B.

4. Discussion

During full forward extrusion, the surface integrity is strongly modified through the ejection process. The increase of grooves on the surface caused by the ejection is directly related to the condition of the extrusion die. In the subsequent deep rolling process, high surface quality was achieved with small rolling overlap $s = 0.05$ mm and high deep rolling force F_{dr} . The larger rolling overlap $s = 0.2$ mm was only used in combination with a reduced deep rolling force—also to keep the height of the waviness profile low. Nevertheless, the spherical path is clearly formed on the surface. For the 100 mm long shoulder, the machining time is equal to $t_{dr} = 100 \text{ mm}/s/n = 100 \text{ mm}/0.05 \text{ mm}/(3981/\text{min}) = 301.5$ s. For industrial applications, the surface quality must be weighed against the long processing time.

An increase in hardness values could only be achieved when the highest pressure and very small rolling overlap were selected. The hardness increase determined for Setup B is negligible. The results of the hardness tests should be viewed with caution, since they are subject to large uncertainties which, even with Setup A, are greater than the average hardness increase achieved. One possibility for a more precise investigation of the hardness development is the microhardness testing of cross-section polishes of the workpieces. However, both cross-section polishes orthogonal to the axial direction and cross-section polishes in the axial–radial plane would eliminate a large portion of the residual stresses.

The residual stress results show that the assumption known from the literature that a significant reduction of residual stresses takes place during ejection also applies to the 16MnCr5 material. Despite the strongly different energy inputs in Setups A and B, the residual stress curves are not significantly different. It appears that even the low plastic deformation of Setup B is sufficient to introduce high compressive residual stresses. A further increase cannot be achieved by Setup A since the material is not able to store the introduced energy. Accordingly, it cannot be assumed that repeated machining of the workpiece by means of deep rolling will lead to a further increase in residual compressive stresses. Regarding the overall objective of increasing fatigue strength, it remains to be verified to what extent the residual compressive stresses tend to rearrange during loading and can actually contribute to an increase in strength.

5. Conclusions

To achieve the overall objective of increasing the strength of impact-extruded 16MnCr5 parts, an experimental study was performed. The development of the surface integrity along the process chain was investigated by means of roughness, residual stress state, and macro-hardness.

1. Using two deep rolling parameter setups, it was shown that an increase in surface finish is possible for the material.
2. With a rolling force of $F_{dr} = 1400$ N, a ball diameter $d_b = 13$ mm, and a step over distance $s = 0.05$ mm, an increase in macro-hardness could also be achieved.
3. In terms of residual stresses, a significant compressive residual stress condition was set at both a rolling force of $F_{dr} = 1400$ N and a rolling force of $F_{dr} = 933$ N.

Since a small amount of energy was applied to the workpiece in one of the tests, it cannot be assumed that a further increase in residual compressive stress can be achieved by further increasing the energy input.

In conclusion, it remains to be shown that the modification of the surface integrity investigated here has a significant effect on the operational behavior of impact-extruded components. The extent to which the residual stress state is maintained during cyclic loading and how the residual stresses are redistributed will have to be investigated.

Author Contributions: Conceptualization, P.H.; methodology, P.H.; formal analysis, P.H., M.M., I.F.W., T.H. and T.B.; investigation, P.H.; resources, T.H. and T.B.; data curation, P.H.; writing—original draft preparation, P.H.; writing—review and editing, P.H., M.M., I.F.W., T.H. and T.B.; visualization, P.H.; supervision, T.H. and T.B.; project administration, T.H. and T.B.; funding acquisition, T.B. All authors have read and agreed to the published version of the manuscript.

Funding: This research was funded by Deutsche Forschungsgemeinschaft (DFG, German Research Foundation), project number 432053466.

Institutional Review Board Statement: Not applicable.

Informed Consent Statement: Not applicable.

Data Availability Statement: Not applicable.

Conflicts of Interest: The authors declare no conflict of interest. The funders had no role in the design of the study; in the collection, analyses, or interpretation of data; in the writing of the manuscript, or in the decision to publish the results.

References

1. Tekkaya, A.E.; Bouchard, P.-O.; Bruschi, S.; Tasan, C.C. Damage in metal forming. *CIRP Ann.* **2020**, *69*, 600–623. [[CrossRef](#)]
2. Schneider, M.J. Introduction to Surface Hardening of Steels. In *ASM Handbook A 4: Steel Heat Treating Fundamentals and Processes*; Dosset, J., Totten, G.E., Eds.; ASM International: Materials Park, OH, USA, 2013; pp. 389–398.
3. Clausmeyer, T.; Schowtjak, A.; Wang, S.; Gitschel, R.; Hering, O.; Pavliuchenko, P.; Lohmar, J.; Ostwald, R.; Hirt, G.; Tekkaya, A.E. Prediction of Ductile Damage in the Process Chain of Caliber Rolling and Forward Rod Extrusion. *Procedia Manuf.* **2020**, *47*, 649–655. [[CrossRef](#)]
4. Wang, X.; Xiong, X.; Huang, K.; Ying, S.; Tang, M.; Qu, X.; Ji, W.; Qian, C.; Cai, Z. Effects of Deep Rolling on the Microstructure Modification and Fatigue Life of 35Cr2Ni4MoA Bolt Threads. *Metals* **2022**, *12*, 1224. [[CrossRef](#)]
5. Chan, W.L.; Cheng, H.K.F. Hammer peening technology—The past, present, and future. *Int. J. Adv. Manuf. Technol.* **2022**, *118*, 683–701. [[CrossRef](#)]
6. Altenberger, I. Deep rolling—The past, the present and the future. In Proceedings of the 9th International Conference on Shot Peening, International Scientific Committee of Shot Peening, Marne-la-Vallée, France, 6–9 September 2005; pp. 144–155.
7. Cherif, A.; Zinn, W.; Scholtes, B. Integration of a Simultaneous Deep Rolling Process in the Heat Treatment of SAE1045 Steel: A Way to Reduce and Optimize the Production Chain. In Proceedings of the 11th International Conference on Shot Peening, International Scientific Committee of Shot Peening, South Bend, IN, USA, 12–16 September 2011; pp. 43–48.
8. Wang, X.; Chen, L.; Liu, P.; Lin, G.; Ren, X. Enhancement of Fatigue Endurance Limit through Ultrasonic Surface Rolling Processing in EA4T Axle Steel. *Metals* **2020**, *10*, 830. [[CrossRef](#)]
9. Dang, J.; An, Q.; Lian, G.; Zuo, Z.; Li, Y.; Wang, H.; Chen, M. Surface modification and its effect on the tensile and fatigue properties of 300M steel subjected to ultrasonic surface rolling process. *Surf. Coat. Technol.* **2021**, *422*, 127566. [[CrossRef](#)]
10. iGF. *Schlussbericht zu IGF-Vorhaben Nr. 18229N: Erweiterung Technologischer Grenzen bei der Massivumformung in Unterschiedlichen Temperaturbereichen*; Forschungsvereinigung Stahlanwendung e.V.: Düsseldorf, Germany, 2018.
11. Oevermann, T.; Wegener, T.; Niendorf, T. On the Evolution of Residual Stresses, Microstructure and Cyclic Performance of High-Manganese Austenitic TWIP-Steel after Deep Rolling. *Metals* **2019**, *9*, 825. [[CrossRef](#)]
12. Meyer, D.; Kämmler, J. Surface Integrity of AISI 4140 After Deep Rolling with Varied External and Internal Loads. *Procedia CIRP* **2016**, *45*, 363–366. [[CrossRef](#)]

13. Hering, O.; Tekkaya, A.E. Damage-induced performance variations of cold forged parts. *J. Mater. Process. Technol.* **2020**, *279*, 116556. [[CrossRef](#)]
14. Hering, O.; Dunlap, A.; Tekkaya, A.E.; Aretz, A.; Schwedt, A. Characterization of damage in forward rod extruded parts. *Int. J. Mater. Form.* **2020**, *13*, 1003–1014. [[CrossRef](#)]
15. Klocke, F. *Fertigungsverfahren 4*; Springer: Berlin/Heidelberg, Germany, 2017.